Research Article

Temitope Love Baiyegunhi*, Kuiwu Liu, Oswald Gwavava, and Christopher Baiyegunhi

Textural characteristics, mode of transportation and depositional environment of the Cretaceous sandstone in the Bredasdorp Basin, off the south coast of South Africa: Evidence from grain size analysis

https://doi.org/10.1515/geo-2020-0135
received May 06, 2020; accepted September 23, 2020

Abstract: A total of 92 representative sandstone samples of the Bredasdorp Basin in boreholes E-AH1, E-AJ1, E-BA1, E-BB1 and E-D3 have been investigated for their grain size characteristics. Grain size textural parameters and their cross plots, linear discriminate functions (LDFs), C–M (C = first percentile and M = median) diagram and log–probability plots were calculated and interpreted to understand the mode of transportation and hydrodynamic conditions and also to unravel the depositional environments of the sediments. The grain size textural parameters revealed that the Bredasdorp sandstones are unimodal, predominantly fine-grained, moderately well-sorted, mesokurtic and near symmetrical. The bivariate plots of grain size textural parameters indicate that the depositional environments had been influenced mainly by river/beach/coastal dune conditions. The LDF plots show that the sediments are turbidity current deposits in a shallow marine environment. The C–M diagram revealed that the studied sandstones were mainly deposited by traction currents and beach process. In addition, the grain size log–probability curves and C–M diagram show the predominance of suspension and saltation modes of sediment transportation. Based on the inter-relationship of the various statistical parameters, it is deduced that the Bredasdorp Basin are mainly shallow marine deposits with signature of beach and coastal river processes.

Keywords: grain size parameters, textural characteristics, hydrodynamic energy, depositional environment, Bredasdorp Basin

1 Introduction

Grain size analysis is a useful tool used by geoscientists on siliciclastic sedimentary rocks in order to obtain a detailed understanding of the hydrodynamic condition and palaeoenvironmental features as well as reconstruct ancient sedimentary transport histories and sediment provenance [1,2]. Grain size distribution is one of the most significant properties of sediment particles because sizes of particles or grains in a particular deposit reveal their hydrodynamic energy and transportation processes [3]. Consequently, grain size analysis reveals some essential evidences of transportation and depositional conditions [2,4]. Also, it is an essential parameter for textural classification of sedimentary rocks [5]. Grain size parameters of clastic rocks also give detailed information on the sediment mode of transportation, sorting and depositional conditions prior to final induration [3,6]. Several researchers [6,7] have documented that indeed each sedimentary environment are thought to have adversely different particle size features that separate them from sediments deposited in other environments.

The particles size distributions directly depend on the transporting medium, duration of transportation, depositional conditions and nature of the environmental setting; and therefore, it has momentous value as an environmental indicator [8]. The size of sedimentary particles can be measured using different methods; however, the choice of techniques depends on the purpose of the studies, the range of grain sizes to be measured and the level of consolidation of sediment or sedimentary rock. Direct sieving and point counting under microscope are some of the widely used methods for grain size determination [9]. The grain sizes in sedimentary rocks that cannot be separated

* **Corresponding author: Temitope Love Baiyegunhi,** Department of Geology, University of Fort Hare, Private Bag X1314, Alice 5700, Eastern Cape Province, South Africa, e-mail: 201814648@ufh.ac.za, lovedestiny324@yahoo.com
Kuiwu Liu, Oswald Gwavava: Department of Geology, University of Fort Hare, Private Bag X1314, Alice 5700, Eastern Cape Province, South Africa
Christopher Baiyegunhi: Department of Geology and Mining, University of Limpopo, Private Bag X1106, Sovenga 0727, Limpopo Province, South Africa

must be measured or determined using any methods except the sieving or sedimentation method [8]. As documented by ref. [8], sedimentologists are generally interested in three major aspects of grain size: (1) procedure for determining particle size and showing it in terms of grain size scale, (2) techniques for summing up large amounts of grain size data and representing them in a graphical and statistical form for easy calculation and (3) the genetic (i.e. environmental) importance of these data. The two main ways of representing grain size data are through graphical and mathematical methods. The graphical method entails plotting the grain size textural data on binary diagram where the cumulative weight percentage nor the individual weight is plotted versus the sieve sizes (in phi units). On the other hand, the mathematical method involves the use of statistical parameters or mathematical expressions to denote the grain size data.

Grain size analysis generates statistical parameters that include the graphic mean, standard deviation, kurtosis and skewness. Pertaining to grain size analysis, the log–probability plots and bivariate diagrams are the two main categories of graphical plots that are commonly used in environmental studies [1,2]. The use of two component grain size variation diagrams, where one statistical parameter is plotted against another (i.e. skewness against kurtosis and skewness vs standard deviation) is supported by refs. [9,10]. The aforementioned bivariate plots supposedly allow the distinction of various environments such as the separation of a river environment from a beach environment as well as other kinds of environments. A number of researchers [2,9,11] have used these bivariate diagrams to establish the areas within which deposits of particular environments can be plotted. Alternatively, quite a number of researchers [12,13] have suggested the use of log–probability plots due to the environmental importance that is related to the shapes of grain size cumulative curve. Visher [12] reported that such curves usually show three or four straight-line segments instead of a single straight line envisaged for a normally distributed population. These straight curve segments are inferred by ref. [12,13] to signify sub-populations of grains transported simultaneously by dissimilar mechanism of transportation (i.e. traction, saltation and suspension). The dissimilarities in the shape of the curves and the location of truncation points of the curve segments supposedly allow demarcation or separation of sediments from different depositional environments. However, while several researchers [2,7] have successfully used the two methods to identify the correct environment, others have failed to effectively distinguish between different environments.

The stratigraphic sequence of the southern Bredasdorp Basin consists of massive feldspathic sandstones, silty sandstones, shaly sandstones, glauconitic sandstones, dark grey shale and mudstones with subordinate and siltstones. Despite the distinct stratigraphic sequence and lithological variation in the Bredasdorp Basin, up to now, no much sedimentological details or information are available about the grain size parameters of the Bredasdorp sandstones. In this study, five offshore exploration wells (Boreholes E-AH1, E-AJ1, E-BA1, E-BB1 and E-D3) located in the Bredasdorp Basin were systematically selected and investigated for grain size analysis (Figure 1). The aim of the study is to interpret the grain size's statistical measures and relate them to their mode of transportation and depositional processes and palaeoenvironment. This study provides the first comprehensive grain or particle size analysis of selected sandstones from the Bredasdorp Basin. The calculated statistical parameters and their inter-relationship, linear discriminate function (LDF) analysis, C–M or Passega diagram and log–probability curves are used to highlight the several aspects of the transportation and depositional conditions the sediment grains underwent as well as relating them to particular depositional environments.

2 General geology and stratigraphy of the Bredasdorp Basin

The continental margin extending along the south coast of South Africa developed during the Mesozoic due to the break-up of Gondwana continent [15]. During this break-up, the continental margin (passive margin) underwent several tectonic events (rift and drift stages) resulting in the formation of the large Outeniqua Basin as well as its sub-basins (Algoa, Bredasdorp, Gamtoos, Pletmos and Southern Outeniqua basins). The Outeniqua Basin developed from dextral shearing processes of South African margin, which started in the early to middle Cretaceous. This basin was reported to have formed along the south coast of South Africa, in response to rift tectonics during the break-up of Gondwana [16] (Figure 1). According to ref. [17], the right-lateral shear or dextral trans-tensional stress movement that was produced along the Falkland–Agulhas Fracture Zone (AFFZ) occurred as a result of the separation of the Mozambique Ridge from the Falkland Plateau as well as the break-up of west Gondwana initiated the development of normal faulting north of the AFFZ, resulting in the creation of graben and half-graben

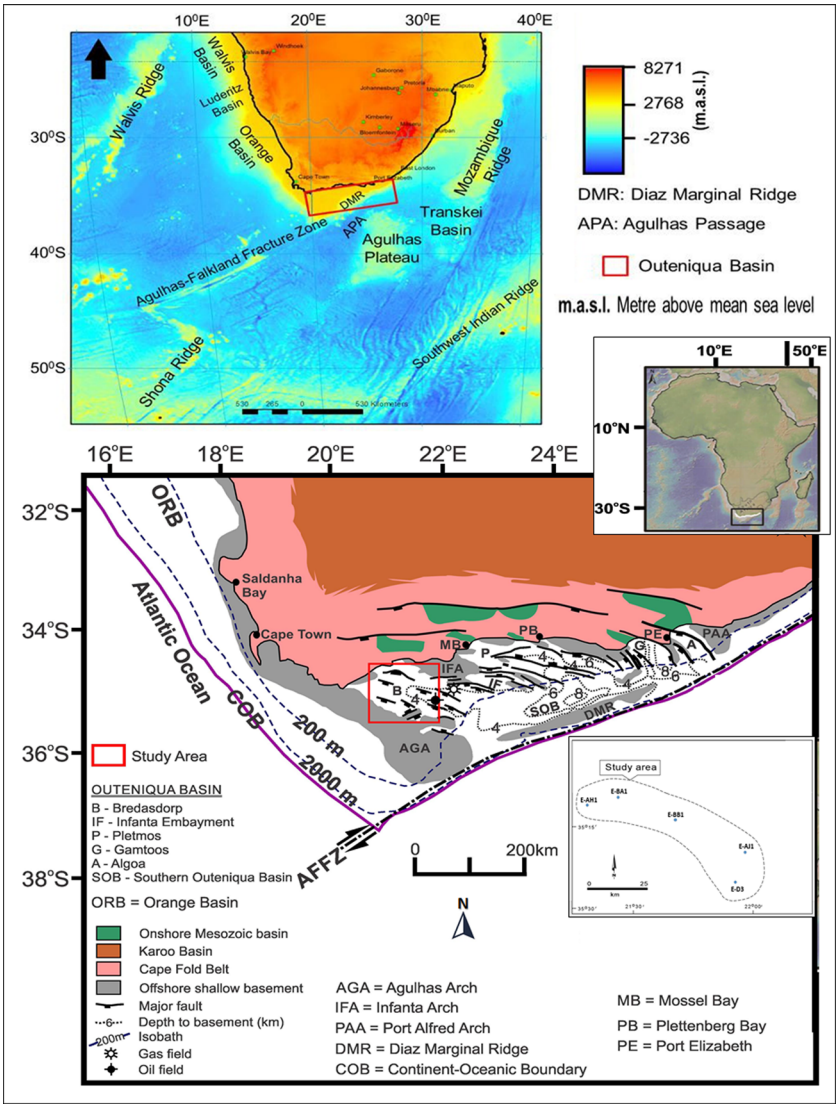

Figure 1: Map of the study area showing distribution of the exploration wells across the Bredasdorp Basin (modified from ref. [14]).

sub-basins including the Bredasdorp Basin [18]. The AFFZ which is the major active fault during the rifting of the large Outeniqua Basin followed the south-easterly pattern of older compressional features of the Permo–Triassic & Cape Fold Belt (CFB). The CFB is a northern verging thrust belt while the AFFZ is a dextral transform fault, forming a boundary between oceanic and continental crusts. The Outeniqua Basin-fill succession is subdivided into a syn-rift sequence and a drift sequence, which is usually associated with passive margin settings. The syn-rift and drift sequences are separated by a regionally developed unconformity referred to as the 1At1, and it took place in the Lower Valanginian time (ref. [19]; Figure 2).

The Bredasdorp Basin which is the focus of this study developed along the South African continental margin, underneath the Indian Ocean during Late Jurassic–Early Cretaceous in response to the extensional periods in the early phases of rifting. This basin is bounded on the western and south-western parts by the Columbine–Agulhas Arch, while the northern part is bounded by the CFB and Infanta Arch. Furthermore, the south-eastern part of the basin is bounded by the Diaz Marginal Ridge (Figure 1). The aforementioned arches are extended basement highs made up of the Cape Supergroup granite and Precambrian metamorphic rocks. The basin has no onshore equivalent despite the fact that it is situated in the middle of two anticlinally predominated basement highs at Cape

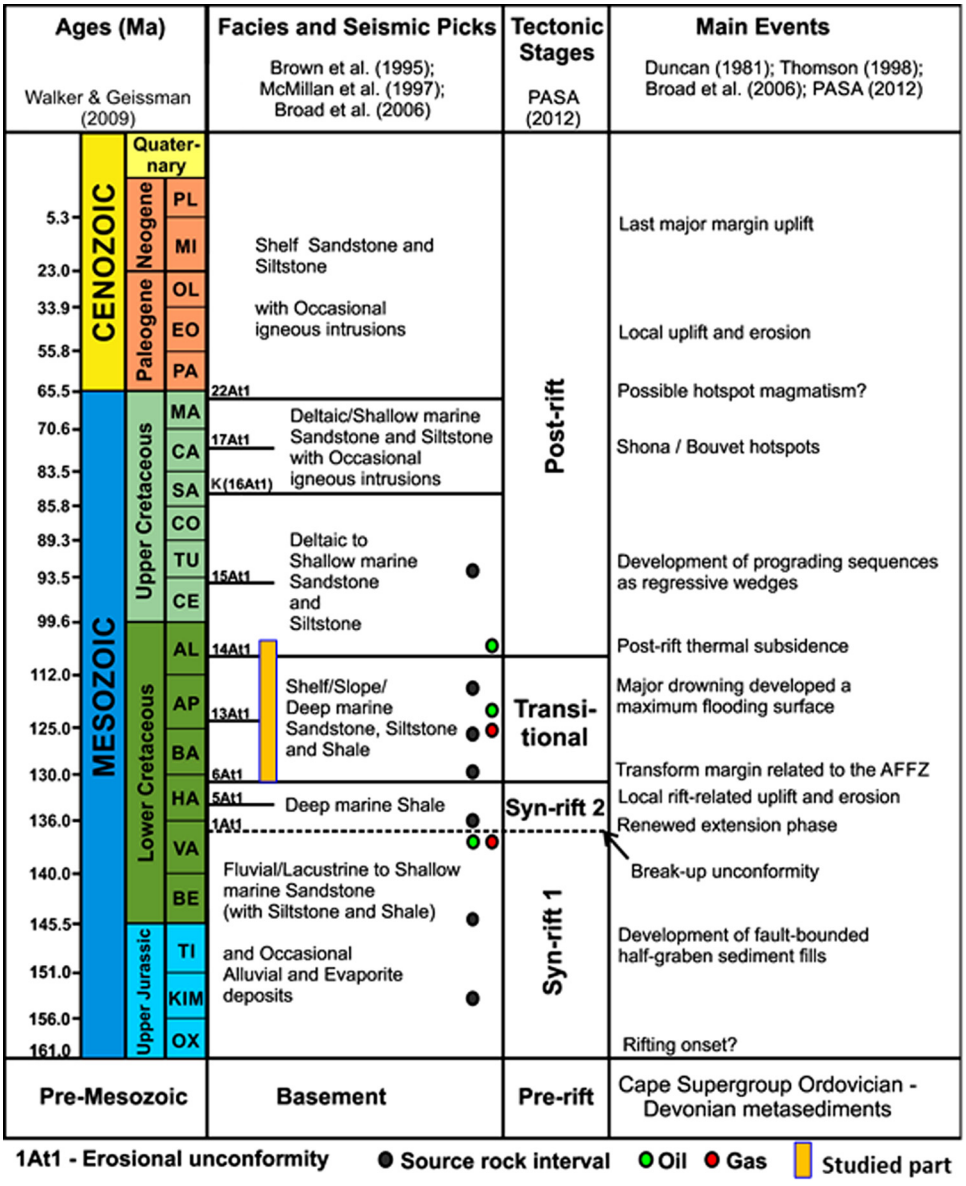

Figure 2: Chrono-stratigraphic chart of the Western Bredasdorp Basin showing main unconformities and tectonic phases relative to geodynamic events [14].

Infanta Agulhas. The Bredasdorp Basin covers an area extent of approximately 15,000 km^2 which is about 100 km in length and 150 km wide [20].

The Bredasdorp Basin as well as the other four sub-basins shows rifted graben as well as half-graben features and are filled with drift sediments of variable thicknesses [19,21]. These half-graben features were reported to have developed when normal faults that dip or tilt towards the same direction make the nearby fault blocks to slide or slip down relative to the fault next to it [22]. Sediments deposition in the Bredasdorp Basin is primarily controlled by the early continental rifting and tectonic development. As reported by ref. [23], the basin serves as a local depocentre and was primarily filled by the late Jurassic – early Cretaceous shallow marine and continental sediments. The deposition of these syn-rift shallow marine and continental sediments continued in the rift system until about 126 Ma, when most of the faulting stopped [21]. So the syn-rift deposition commenced and subsequently initiated a transitional phase and, thereafter, a drifting phase [24].

The tectonic evolution of the Bredasdorp Basin can be categorized into rift phase (syn-rift 1 and syn-rift 2), early drift or transitional phase and the post-rift or drift phase (Figure 2). The rift phase is characterized by extension-instigated subsidence and syn-rift basin fill. The

isostatic uplift of both sides of the half-graben led to the erosional distortion of the late-rift sediments, whereas the great marginal uplift and erosion of the northern side removed the whole syn-rift sequence in some places [21]. The rift phase can be subdivided into the syn-rift and post-rift sequence. The syn-rift sedimentary sequence consists of shallow marine and fluvial sediments, while the post-rift or drift sequence is made up of deep marine sediments [19,25]. The post-rift successions represent a set of stratigraphic units and their deposition is related to the early and late episodes of the steady west-southwest-ward plate movements of the southern coast of Africa. These movements resulted in the formation of the Outeniqua sub-basins. The early drift phase occurred just before the onset of rapid thermal subsidence; and it is associated with continued uplift, resulting in erosion truncation on the southern edges. Fast subsidence and deposition of the deepwater sediments took place within the graben [21]. The drift phase is characterized by a regional subsidence that was compelled by sediment loading and thermal cooling. Continued subsidence (minor) up to the early Tertiary, when alkaline intrusive disturbed the southern side, led to uplift and erosion [21].

The Bredasdorp Basin is envisaged to host an Oxfordian-Recent stratigraphic column that overlies the rocks of the Cape Supergroup [24]. The late Jurassic to early Cretaceous shallow marine and fluvial syn-rift deposits are first to be deposited and they underlie the Albian to Recent shallow marine sediments [21]. The stratigraphic column shows the existence of a middle Jurassic to early Cretaceous syn-rift phase, and it is subsequently overlain by the early Cretaceous to Tertiary post-rift phase [21]. The syn-rift sedimentation phases of the Bredasdorp Basin are subdivided into the syn-rift I and syn-rift II phases [21]. According to ref. [21], the syn-rift I phase occurred in the middle Jurassic–late Valanginian (Basement up to 1At1), whereas the syn-rift II took place in the Late Valanginian–Hauterivian (1At1 to 6At1). The syn-rift I succession is terminated by the 1At1 regional unconformity. This 1At1 unconformity signifies the beginning of a renewed rifting (syn-rift II) phase initiated due to early or initial movement along the AFFZ at approximately 121 Ma (Valanginian–Hauterivian boundary) [21]. The syn-rift II was later followed by the transitional (early drift) phase, which occurred during Hauterivian–early Aptian (6At1 to 13At1; Figure 2). The transitional (early drift) phase was dominated by recurrent episodes of progradation and aggradation, and it was mostly affected by tectonic events and eustatic sea-level changes [21,26]. The transitional (early drift) phase was considered as the first deepwater deposits in the Bredasdorp Basin and they were deposited due to major subsidence of the basin as well as the increase in water depth. On the other hand, the late drift phase trailed a major marine regression in the Bredasdorp Basin during the early Aptian. This regression event resulted in a major erosion which is marked by the 13At1 unconformity. The erosion period is followed by a marine transgression, which carried and deposited organic-rich mudstone, shale or claystone in the basin under an anoxic condition [24]. The onset of the late drift phase is manifested or noted by the 14At1 mid-Albian unconformity (Figure 2), which marks the beginning of the active thermally instigated subsidence when the Columbine–Agulhas Arch was cleared by the trailing edge of the Falkland Plateau in the late Albian [26].

3 Materials and method

Grain size data are presumed to be useful in construing the depositional environments of long laid siliciclastic sedimentary rocks. In this study, 92 representatives' thin sections of different sandstone types from five exploration wells (boreholes E-AH1, E-AJ1, E-BA1, E-BB1 and E-D3) were selected systematically to cover textural variations (i.e. grain size, shape and arrangement). The selected exploration wells are situated in the central to southern section of the Bredasdorp Basin and geographically located between latitudes 35°00′ S and 35°30′ S and longitude 21°00′ E and 22°00′ E (Figure 1 and Table 1).

The stratigraphic column showing where the samples were collected is presented in the supplementary data (Figure S1). The selected sandstone samples were investigated for their grain size textural parameters and statistical relationships. Generally, particle size distribution in consolidated sedimentary rocks can be more accurately determined by measuring grains in thin sections under petrographic microscope with an inbuilt ocular micrometer (microscopic method). The aforementioned method is better than the traditional way of estimating the size and sorting of sand- and silt-size particles using a reflected-light binocular microscope and a standard size-comparison set, consisting of grains of specific sizes mounted on a glass or card. The microscopic method tends to yield grain sizes that are smaller than the highest diameter of the grains due to the fact that the plane of a thin section does not cut precisely through the centres of most grains. Hence, grain sizes measured using the thin-section method are usually corrected mathematically to make them agree with the sieve data [27]. The thin section or microscopic method

Table 1: Coordinates and total drilling depth of the exploration wells studied

Wells/borehole	E-AH1	E-AJ1	E-BA1	E-BB1	E-D3
Coordinates	Latitude 35°11′ 13.40″ S Longitude 21°08′ 37.07″E	Latitude 35°20′ 09.15″ S Longitude 21°58′ 37.45″E	Latitude 35°09′ 29.67″ S Longitude 21°28′ 31.19″E	Latitude 35°14′ 51.32″ S Longitude 21°41′ 41.088″E	Latitude 35°28′ 45.91″ S Longitude 21°56′ 16.16″E
KB to sea level (m)	26	26	22	22	18
Water depth (m)	91	142	115	122	156
Total drilling depth (m)	3,729	3,490	3,130	3,320	3,996
No. of samples	8	27	11	38	8

N.B: Kelly Bushing (KB) represents the vertical distance from the Kelly bushing device on rigs down to the sea level.

technique involves the subdivision of the sediments into different size fractions, allowing the construction of grain size distribution from the weight percentage of sediment in individual size fraction. In this study, grain size analysis was carried out on the thin sections under a petrographic microscope with an inbuilt ocular millimetre scale. A minimum of 500 grains were measured per thin section by using the standard method of measuring the grain's longest axis [27]. Grains in sedimentary rocks depict a wide range of size distributions; hence the frequencies of grain size ranges were computed, and the Udden–Wentworth grade scale was used to determine the grain size classes. The unit of grain sizes (millimetres) was changed to a phi scale using the expression below:

$$\varnothing = -\log_2 D,$$

where $\varnothing$ and D represent the phi size and grain diameter (in millimetres), respectively.

The obtained grain size data were presented as frequency histograms and cumulative frequency curves. Since the sorting and mean grain size of the studied sandstones cannot be directly measured, mathematical methods that permit statistical processing of grains size data were extracted or obtained from the cumulative frequency curves as shown in Figure 3 in order to mathematically define the grain size distribution.

In clastic sedimentary rocks, certain standard statistical measures were usually described for grain size distribution, and these can be subdivided into four main parameters, including the graphic mean, graphic standard deviation, graphic skewness and graphic kurtosis (KG). The mean grain size shows the central tendency, average grain size or class of the sediment. It is translated in terms of the available energy as the average velocity or kinetic energy of the depositing media. Standard deviation accounts for the uniformity or sorting of sediments and reveals the variations in the velocity or kinetic energy conditions of the depositing medium about its average velocity. For instance, when a sediment is produced by a combination of two different modes of deposition (bed load and suspended load), the standard deviation shows the difference in the kinetic energy (velocity) associated with their modes of deposition. The graphic skewness (SK_i) measures the symmetrical of the grain size distribution (i.e. predominance of coarser or fine sediments) and marks the position of the mean with respect to the median. A symmetrical curve with excess coarse material will have a negative value, while the one with excess fine material indicates a positive value; a zero value is indicated by a symmetrical curve. Alternatively, a positive skew indicates an abundance of coarse grains with a tail in the direction of the fines, while a negative skew indicates an abundance of fines with a tail in the direction of the coarse sediments. The kurtosis (KG) is traditionally defined as a measure of the peakedness or sharpness of a frequency cumulative curve [27]. On the contrary, Kendall and Stuart [28] reported that this definition or expression is not totally correct. Hence, kurtosis should not be defined in terms of the shape (flatness or peakedness) of the frequency curves. Instead, it should be interpreted or defined as the ratio of sorting within the central 90% of the distribution to the sorting of the central 50%. For that reason, kurtosis measures the sorting ratio rather than peakedness of the frequency curves. In cases where the tails are better sorted than the central parts, then it is referred to as platykurtic; and when the central part is better sorted, it is known as leptokurtic. Furthermore, if the tail and the central part are both equally sorted, then it is called mesokurtic. Detailed information or definition of the aforementioned statistical parameters are documented in ref. [5]. These statistical parameters were calculated using the equation proposed by Johnson [29] (Table 2). The verbal interpretation of the textural parameters is presented in Table 3.

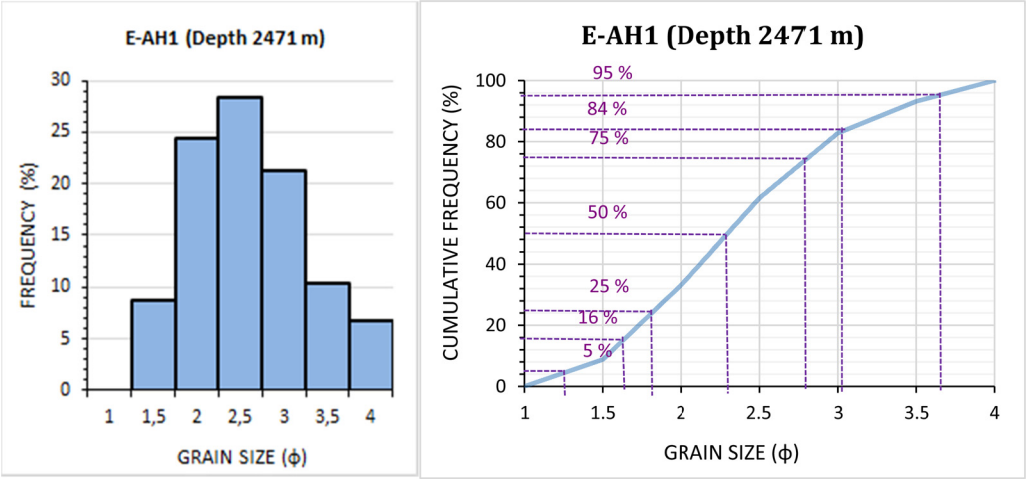

Figure 3: Graphical representation of how statistical parameters were derived from grain size frequency histogram (left) and cumulative frequency curve (right).

Different bivariate scatter plots of the statistical parameters were used to distinguish between depositional settings based on the variations in the textural characteristics of the sandstones. In addition, the LDF mentioned by Sahu [31] was improved and used to discriminate between transportation processes and depositional environments. Likewise, grain size textural parameters, modified C–M pattern in ref. [32] and log–probability curves proposed by Visher [12] were employed to unravel the depositional processes and the mode of transportation.

4 Results and discussion

4.1 Grain size statistics

The grain size cumulative frequency curves for the analysed samples reveal that all the studied samples are unimodal in nature with peaks mostly at 2.5∅ and a few at 3.0∅ and 3.5∅ (Figures S2 and S3 in the supplementary data) and mostly show near symmetrical distribution (Table S1 in the supplementary data). The unimodality of the studied sandstones indicates the consistent or steady depositional process during which the sediments were settled. In addition, the occurrence of most peaks at 2.5∅ as well as the unimodality characteristics perhaps reveals low-energy condition of roughly uniform nature during the deposition of the sediments. The fairly wide and gentle sloping nature of the cumulative curves indicate relatively low kinetic energy and velocity regime of the depositing media. Considering the fact that the size of the sediments is controlled by two main factors, namely, the energy of the medium and the particle sizes of the sediments, the range of the grain sizes (0.5∅ up to 4.0∅) generally indicates fine to medium sediments. The fine to medium nature of the sediments can be attributed to somewhat lower energy condition and less velocity variation in the medium. Likewise, the presence of fine skewed distribution in four of the five studied boreholes indicates that finer fraction is ample in the depositional environment. Since there is no abrupt change in grain sizes, it may be inferred that wide upliftment or subsidence covering both the source area and depositional area took place.

Table 2: Formulas for graphical calculation of grain size parameters [29]

Graphic mean (M_z)	$M_z = \frac{\varnothing_{16} + \varnothing_{50} + \varnothing_{84}}{3}$
Graphic standard deviation (σ_i)	$\sigma_i = \frac{\varnothing_{84} - \varnothing_{16}}{4} + \frac{\varnothing_{95} - \varnothing_5}{6.6}$
Graphic skewness (SK_i)	$SK_i = \frac{(\varnothing_{84} + \varnothing_{16} - 2\varnothing_{50})}{2(\varnothing_{84} - \varnothing_{16})} + \frac{(\varnothing_{95} + \varnothing_5 - 2\varnothing_{50})}{2(\varnothing_{95} - \varnothing_5)}$
Graphic kurtosis (KG)	$KG = \frac{(\varnothing_{95} - \varnothing_5)}{2.44(\varnothing_{75} - \varnothing_{25})}$

The 5th, 16th, 25th, 50th, 75th, 84th and 95th percentile on the cumulative frequency curve is represented by $\varnothing_5$, $\varnothing_{16}$, $\varnothing_{25}$, $\varnothing_{50}$, $\varnothing_{75}$, $\varnothing_{84}$ and $\varnothing_{95}$, respectively.

4.2 Textural characteristics

The studied sandstones are generally fine- to medium-grained and moderately sorted to moderately well-sorted (Figure 4). Specifically, borehole E-AH1 mostly consists of massive, well-sorted, fine- to medium-grained glauconitic

Table 3: Textural parameters and their corresponding verbal terms [30]

Standard deviations (σ_1)		Skewness (SK_i)		Kurtosis (KG)	
Phi standard deviation	**Verbal sorting**	**Calculated skewness**	**Verbal skewness**	**Calculated kurtosis**	**Verbal kurtosis**
<0.35∅	Very well-sorted	>0.30	Strongly fine skewed	<0.67	Very platykurtic
0.35–0.50∅	Well-sorted	0.30–0.10	Fine skewed	0.67–0.90	Platykurtic
0.50–0.71∅	Moderately well-sorted	0.10 to −0.10	Near symmetrical	0.90–1.11	Mesokurtic
0.71–1.00∅	Moderately sorted	−0.10 to −0.30	Coarse skewed	1.11–1.50	Leptokurtic
1.00–2.00∅	Poorly sorted	<−0.30	Strongly coarse skewed	1.50–3.00	Very leptokurtic
2.00–4.00∅	Very poorly sorted			>3.00	Extremely leptokurtic
>4.00∅	Extremely poorly sorted				

sandstone and claystone with minor siltstone interbeds. Borehole E-AJ1 is made of claystones and siltstones with occasional interbedded sandstones. The sandstones in borehole E-AJ1 are generally massive (structureless), fine- to medium-grained and contain abundant glauconite and are moderately well-sorted. Borehole E-BA1 mostly comprises massive moderately well-sorted, fine- to medium-grained glauconitic sandstone with minor claystone and siltstone. The sandstone is slightly porous, light brownish-grey with very fine to medium, well-sorted subangular grains. In addition, it is non-calcareous, slightly glauconitic and slightly pyritic and contains green lithic fragments. The sandstone in borehole E-BB1 is mostly well-sorted, fine-grained, glauconitic and slightly shelly. In borehole E-D3, the sandstones are moderately sorted, medium-grained, and slightly glauconitic. In general, the roundness of the grains in the studied sandstone samples vary from subangular to rounded and the sphericity ranges from low to high (mostly low; oblong grains). The grain packing is irregular, showing both fairly packed and tightly packed grains. However, in most cases, the grains are moderately tight.

4.3 Textural parameters

A series of textural parameters can be calculated for any grain size distribution curve. In this research work, the four statistical parameters used to depict the textural characteristics of the Bredasdorp sediments are the median, mean (M_z), standard deviations (σ_1), skewness (SK_1) and kurtosis (KG); Figures S4–S8 in the supplementary data.

4.3.1 Graphic mean grain size (M_z)

The mean grain size of the Bredasdorp samples is presented in the supplementary data (Table S1). The calculated mean values for the Bredasdorp samples in Boreholes E-AH1, EAJ1, E-BA1, E-BB1 and E-D3 range between 1.33∅ and 2.33∅, 1.32∅ and 3.31∅, 1.28∅ and 3.31∅, 1.19∅ and 3.29∅ and 2.31∅ and 3.29∅, respectively. Furthermore, the average mean grain size values in Boreholes E-AH1, E-AJ1, E-BA1, E-BB1 and E-D3 are 1.95∅, 2.18∅, 2.17∅, 2.19∅ and 3.20∅, respectively. These average values show the predominance of fine sand category, but each borehole still shows local variations, varying from medium to fine-grained sands. The massive sandstones, silty sandstones and shaly sandstones are medium, fine and very fine-grained, respectively. Generally, the observed changes in the mean grain size is due to instabilities in the energy condition during the deposition of sediments. The fine-grain nature perhaps revealed the moderately low-energy condition in the basin at the time of deposition. On the other hand, the intermittent occurrence of the medium-grained sand (massive sandstone) could be as a result of limited inputs and sudden increase in the energy conditions [9].

4.3.2 Graphic standard deviations (σ_1)

The standard deviation values of the studied samples range from 0.50∅ to 0.86∅ (Table S1 in the supplementary data) in the variable scale of ref. [30], indicating moderately well-sorted to moderately sorted. Specifically, shaly sandstones are moderately well-sorted, whereas the silty and massive sandstones are moderately well-sorted to

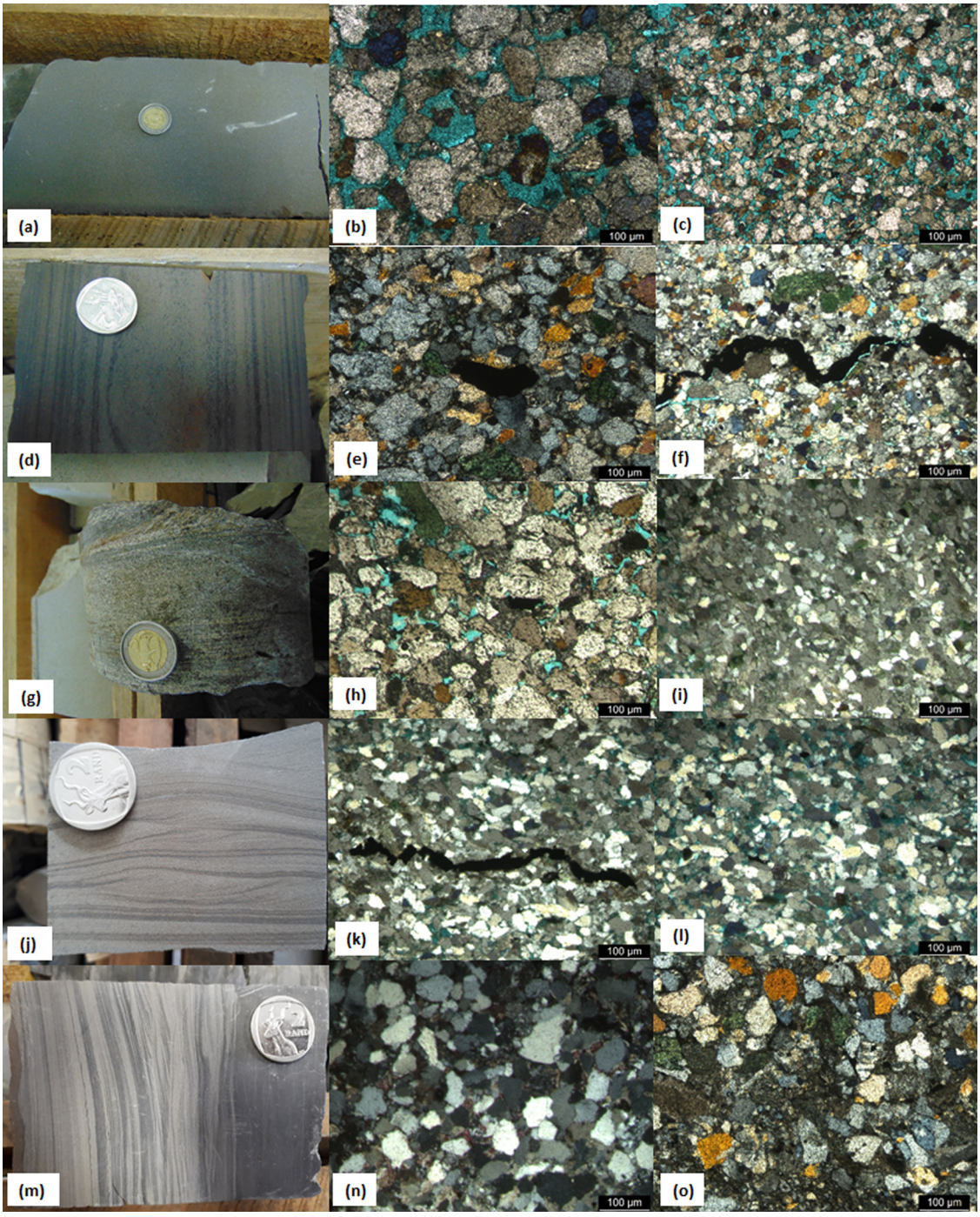

Figure 4: (a) Photograph of massive and fine- to medium-grained sandstone in borehole E-AH1. (b and c) The thin-section photomicrograph of the sandstone from borehole E-AH1 showing pore spaces and glauconite. (d) Photograph of massive and fine- to medium-grained sandstone in borehole E-AJ1. (e and f) The thin-section photomicrograph of the sandstone from borehole E-AJ1 showing that the grains are moderately sorted. (g) Photograph of faintly laminated to massive sandstone in borehole E-BA1. (h and i) The thin-section photomicrograph of the sandstone from borehole E-BA1 showing that the sandstone is fine- to medium-grained and moderately well-sorted. (j) Photograph of ripple laminated sandstone in borehole E-BB1. (k and l) The thin-section photomicrograph of the sandstone from borehole E-BB1 showing that the sandstone is well-sorted, fine-grained and glauconitic. (m) Photograph of ripple laminated sandstone in borehole E-D3. (n and o) The thin-section photomicrograph of the sandstone from borehole E-D3 showing that the roundness of the grains vary from subangular to rounded.

moderately sorted. All the samples from Boreholes E-AH1, E-BA1 and E-D3 are moderately well-sorted, ranging from 0.56∅ to 0.71∅. Most of the samples in the Borehole E-BB1 are moderately well-sorted except for two samples (samples taken at a depth of 3,282 and 2,539 m) that fall in the moderately sorted category, ranging from 0.71∅ to 0.72∅. In the Borehole E-AJ1, of the 27 samples, 20 samples are moderately well-sorted, ranging from 0.50∅ to 0.70∅; whereas the remaining 7 samples are moderately sorted ranging from 0.72∅ to 0.86∅. In general, the predominance of moderately well-sorted sediments could be due to repeated back and forth movement or winnowing action by the depositing agent as well as additional incursion of hitherto sorted sediments in the depositional environment [2,32].

4.3.3 Graphic skewness (SK_1)

The calculated graphic skewness values for the samples vary from −0.22 to 0.16 (Table S1 in the supplementary data), indicating coarse skewed to fine skewed. The shaly sandstones are near symmetrical, while the silty and massive sandstones are fine to coarse skewed. Of 92 samples from the Boreholes E-AH1, E-AJ1, E-BA1, E-BB1 and E-D3, 72 are near symmetrical (−0.08 to 0.09), 17 are fine skewed (0.10 to 0.16) and 3 are coarse skewed (−0.22 to −0.10). The calculated skewness values vary between negative and positive values, showing the presence of both finer and coarser fractions. Generally, the presence of near symmetrical and fine skewed sediments marks the beginning of deposition of fine materials and removal of coarser portion. These near symmetrical sediments suggest moderate energy condition in the depositional environment, whereas the fine skewed sediments suggest much winnowing or longer transportation of the sediments [33]. The dominance of the near symmetrical nature of sediments could be due to the lack of extreme conditions such as wave breaking, tidal variations and seasonal supply of detrital materials.

4.3.4 Graphic kurtosis (KG)

The KG values for the studied samples range from 0.87 to 1.21, which falls in the platykurtic to leptokurtic category (Table S1 in the supplementary data). The silty sandstones are mesokurtic to leptokurtic, whereas the shaly and massive sandstones are platykurtic to mesokurtic. The KG values in Boreholes E-AH1, E-AJ1, E-BA1, E-BB1 and E-D3 vary between 0.90 and 1.05 (mesokurtic), 0.91 and 1.21 (mesokurtic to leptokurtic), 0.92 and 1.08 (mesokurtic), 0.87 and 1.07 (platykurtic to mesokurtic) and 0.88 and 0.95 (platykurtic to mesokurtic), respectively. Most of the samples have mesokurtic category (82 samples), followed by platykurtic (7 samples) and leptokurtic (3 samples). The mesokurtic to leptokurtic nature of the studied samples points to the incessant addition of finer fractions or materials after the winnowing action of the depositing agent and preservation of their original or initial characters during deposition. The dominance of mesokurtic character shows that the better sorted sediments were laid down by one-directional flow of current, allowing the sediments to settle in the lower energy environment [33]. Likewise, the leptokurtic character of the studied samples also signifies the fluctuations in the energy conditions during deposition [8]. The variations in kurtosis values are as a result of variations in the flow characteristics of the transportation and depositional medium. The presence of fine sand-size particles of mesokurtic to platykurtic characteristics as well as the roundness of the grains shows maturity of the sands, which are possibly due to the build-up of fine sand-size materials in a prevailing low-energy environment.

4.4 Inter-relationship of the textural parameters

Understanding the inter-relationships between different textural parameters is important when identifying mechanisms and distinguishing between different depositional environments because sediments textural parameters are environmentally sensitive [2,7]. Several researchers [2,9, 34–37] have used and reported that binary or cross plots of textural parameters of particle size data are reliable tools for distinguishing between different depositional processes as well as unravelling the depositional environments. The bivariate plots of textural parameters are founded on the notion that textural parameters consistently reveal differences in the fluid-flow modes of transportation and deposition of the sediments [36]. Al-Ghadban [35] documented that the most vital and the frequently used bivariate plots are mentioned by refs. [9,11,34]. Stewart [34] proposed that the river process, wave process and slow settling in quiet water could be successfully separated using a bivariate plot of the standard deviation vs skewness. In addition, Moiola and Weiser [11] reported that beach and river sediments could be differentiated by using the bivariate

or cross plot of standard deviation vs skewness, whereas the dune and river sediments could be discriminated using the binary plot of standard deviation against mean. These aforementioned plots have also been attempted for the Bredasdorp sandstones to differentiate between different beach and river environment. The cross plot of skewness vs standard deviation, standard deviation against mean, kurtosis vs skewness and skewness against mean was employed to differentiate between the various depositional processes and environment.

4.4.1 Graphic standard deviation vs mean size

The binary plot of the graphic mean size against standard deviation (sorting) revealed that the studied samples are very fine to medium sand and are moderately sorted to moderately well-sorted. Majority of the Bredasdorp sandstones are moderately well-sorted and fine-grained, indicating that the samples had an equitable time in the transporting medium; and due to the grain to grain interaction, the grain sizes perhaps reduced. The dominance of the moderately well-sorted signifies the continuous or uninterrupted reworking of the Bredasdorp sediments by currents and wave processes [2]. The overall impression of the Bredasdorp sediments is unimodal, with the fine sand as the dominant constituent. The few medium sand is subordinate, making the admixture to moderately well-sorted to moderately sorted. In terms of the depositional environment, the binary plots of standard deviation vs mean (Figure 5) show the influence of both the beach and riverine environment. In addition, Figure 5c shows the gathering of samples near the far end of right limb of the inverted V-shaped background pattern mentioned by Folk and Ward [29], suggesting the dominance of lesser size range of the grains. As reported by Griffiths [38], the mean grain size and the sorting of the samples are controlled hydraulically, such that in all sedimentary environments, the well-sorted and moderately well-sorted sediments have average grain size in the fine sand-size range.

4.4.2 Graphic mean size vs skewness

The binary plot of skewness against mean revealed that the Bredasdorp sandstones are mostly near symmetrical and fine-grained (Figure 6a). Also, Figure 6b shows that the samples plotted or gathered inside the sinusoidal model curve proposed by Folk and Ward [29], indicating the dominance of grains of smaller size range. The sinusoidal nature of the studied samples is as a result of the nearly equal admixture of two size classes (i.e. fine sands and medium sands) of the sediments. Again, this is in agreement with the inverted V-shaped curve in Figure 5c as proposed by Folk and Ward [29]. Overall, unimodal sediments are nearly symmetrical but the mixing produces either fine or coarse skewness subject to the proportions or ratios of grain size classes in the admixture. The cross plot of skewness vs mean (Figure 6c) shows that the samples plotted in the coastal and dune environment mentioned in refs. [11] and [39]. But Bredasdorp sandstones are more likely or possibly of coastal dune than desert dune. Also, reasonable number of samples clustered in the fields of wave and river processes proposed by Stewart [34], with the wave processes dominating. This bivariate diagram shows overlapping of plots, perhaps indicating a multiple influence of river, dune and beach environmental conditions [4].

4.4.3 Graphic mean size vs kurtosis

The binary plot of graphic mean vs kurtosis shows that the studied sandstones are very fine to medium-grained and platykurtic to leptokurtic, with the mesokurtic character dominating (Figure 7a). The plot of kurtosis against mean (Figure 7b) depicts the scattering of the samples close to the bottom, along the normal KG curve section of the established trend of Folk and Ward [29]. This model plot of Folk and Ward [29] shows three gathering or clustering groups of the samples along the normal curve, perhaps pointing to the mixing of three grain size classes, which mostly affected the standard deviation (sorting) in peak and tails and the inverted "V" pattern. The grain mixture is mainly fine sands and lesser amount of medium and very fine sands. The proportionate or nearly equal grain mixture resulted in the good sorting, varying between moderately well-sorted and moderately sorted. The variable proportions of very fine- and medium-grained sediments mixed with predominant fine-grained sand reduced the degree of sorting, especially in the tails; thus, leptokurtic to platykurtic conditions occurred.

4.4.4 Graphic skewness vs standard deviation

The binary plot of the graphic skewness vs standard deviation indicates that the Bredasdorp sandstones are mostly moderately well-sorted and have near symmetrical character (Figure 8a). Furthermore, Figure 8a reveals the dominant influence of the beach environment. However, the

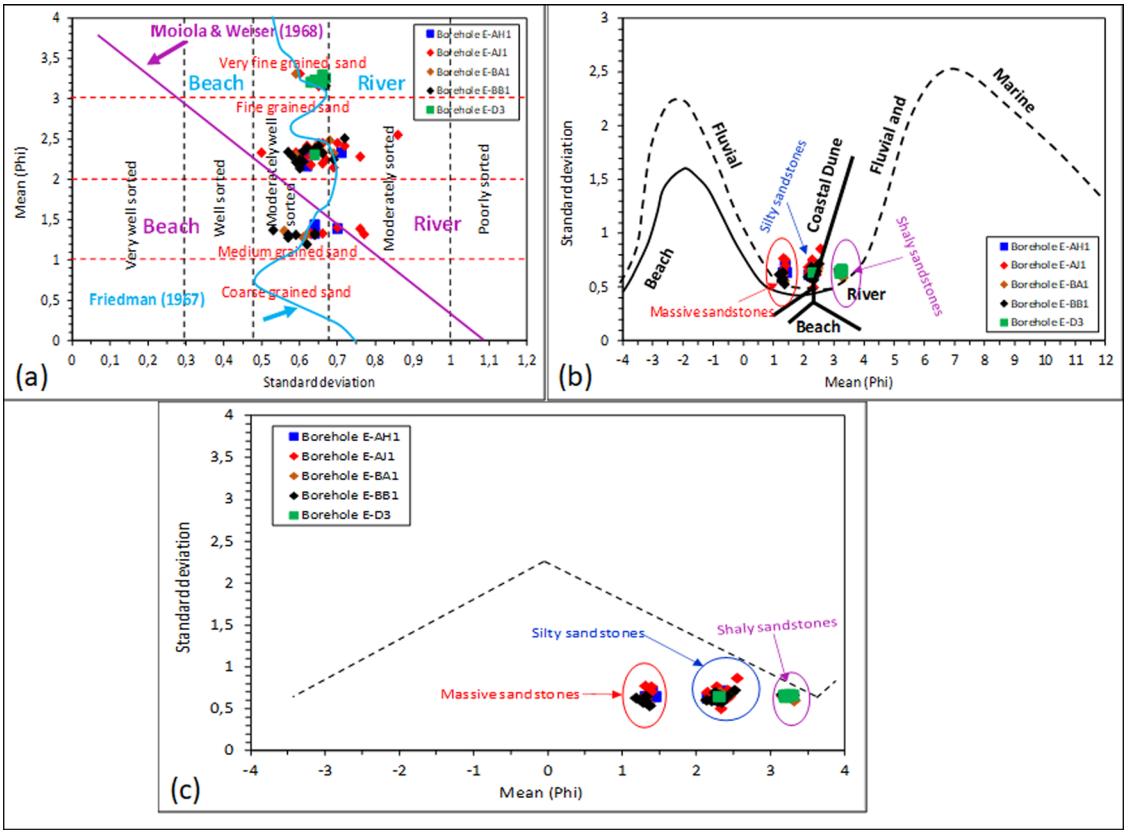

Figure 5: Binary plot of standard deviation against mean skewness showing the environment of deposition. (a) Background pattern [9,11,30]. (b) Background pattern [29]. (c) Placement of the samples in the model plot proposed by Folk and Ward [29]. Note: the fields of beach, dune and river, environments in (b) are modified from ref. [9]. The massive and silty sandstones indicate coastal dune environments, whereas the shaly sandstones support river environment.

modified proposed model plot mentioned in ref. [9] (Figure 8b) shows the clustering of grains in two sectors, perhaps as a result of the combination of two modes of almost the same proportion in bimodal sediments. The minor proportion of grains finer or lesser than sand class is manifested in the binary diagram (Figure 8b) slightly outside the pure sand region of the model proposed by Folk and Ward [29]. The skewness values deviate from the dominant near symmetrical category into the fine and coarse skew category due to the fact that the prevalence sand mode having subordinate silt mode. The bivariate plot (Figure 8b) points to the dominance of dune sedimentation followed by beach and river deposits.

4.4.5 Graphic skewness vs kurtosis

The cross plot of skewness vs kurtosis of a particular sediment population is a useful statistical parameter for differentiating between various environments of deposition [9]. The binary plot of skewness against kurtosis shows that the Bredasdorp samples are mostly near symmetrical and are leptokurtic to platykurtic (Figure 9a). Also, in terms of the depositional environment, Figure 9a shows the influence of mainly riverine environment. As reported by Friedman [39], extremely low or high kurtosis values suggest that a section of the sediments attained their sorting somewhere else in a high-energy environment. The binary plot of skewness vs kurtosis follows a normal path of sinusoidal trend as the mean size varies and is reliant on two modes ([29]; Figure 9b). Generally, as shown in Figure 9b, the studied samples fall in the normal curve or shaded area of the proposed model of Folk and Ward [29], representing the almost pure sand and sand–silt mixture.

4.5 Linear discriminate function (LDF)

The usage of LDFs as a tool in interpreting the changes in energy and fluidity factors during sediment deposition

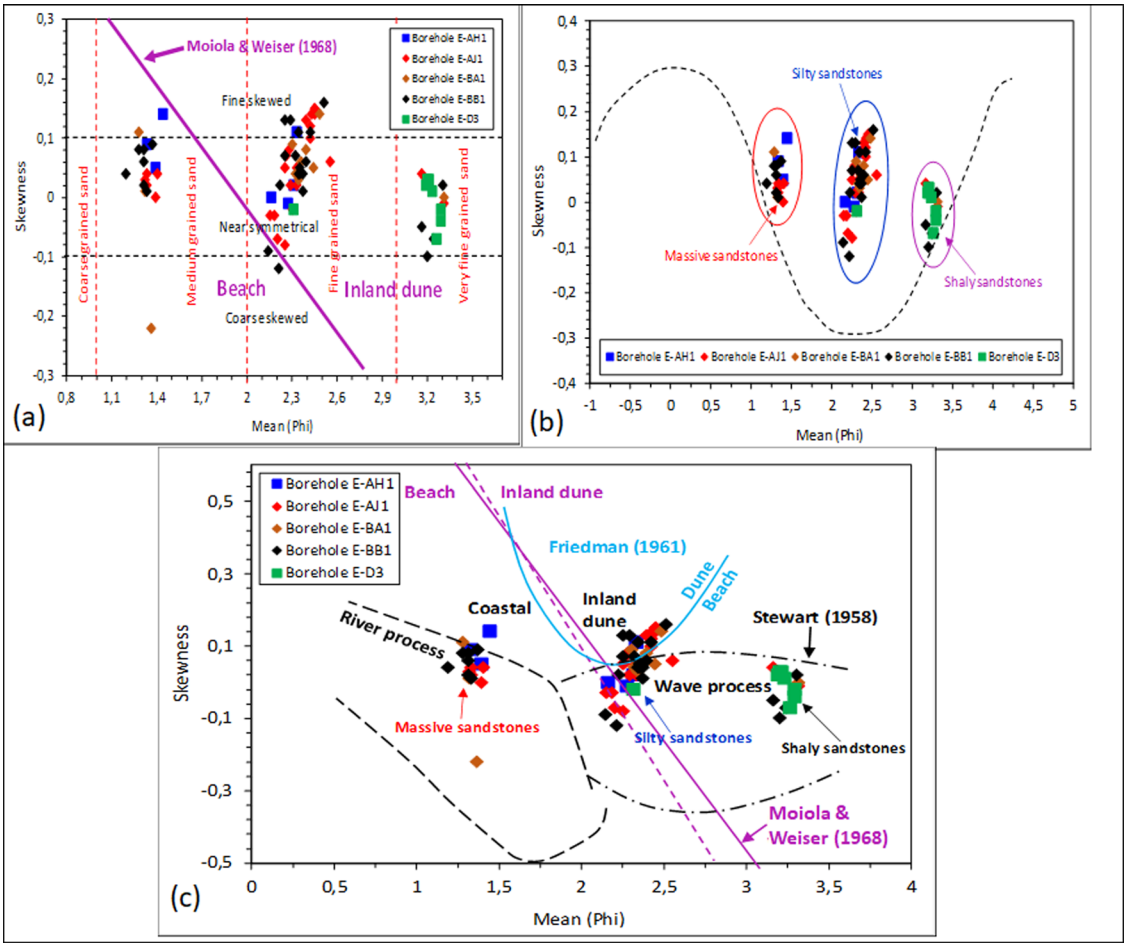

Figure 6: Bivariate plot of mean size vs skewness of sandstones from the Bredasdorp Basin showing (a) grain sizes, skewness and depositional environment (background map [11,39]); (b) placement of the studied samples in the sinusoidal model curve [29]; (c) coastal dune, wave and river processes (background map [11,34,39]). Note: The medium-, fine- and very fine-grained sands are the massive, silty and shaly sandstones, respectively.

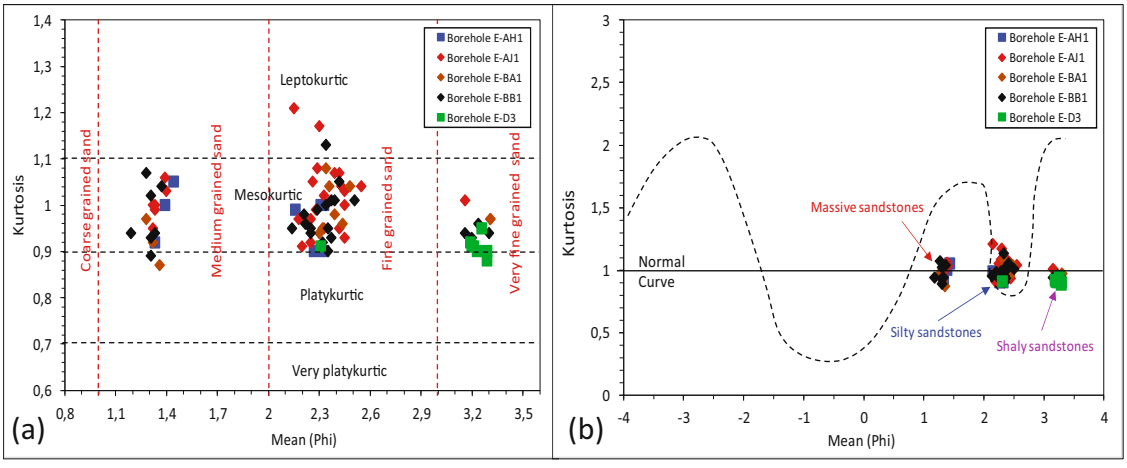

Figure 7: Bivariate plot of mean size versus kurtosis for the Bredasdorp sandstones, showing (a) grain sizes, kurtosis category and depositional environment (background map [11,30]) and (b) placement of the samples in the normal curve model plot proposed by Folk and Ward [29].

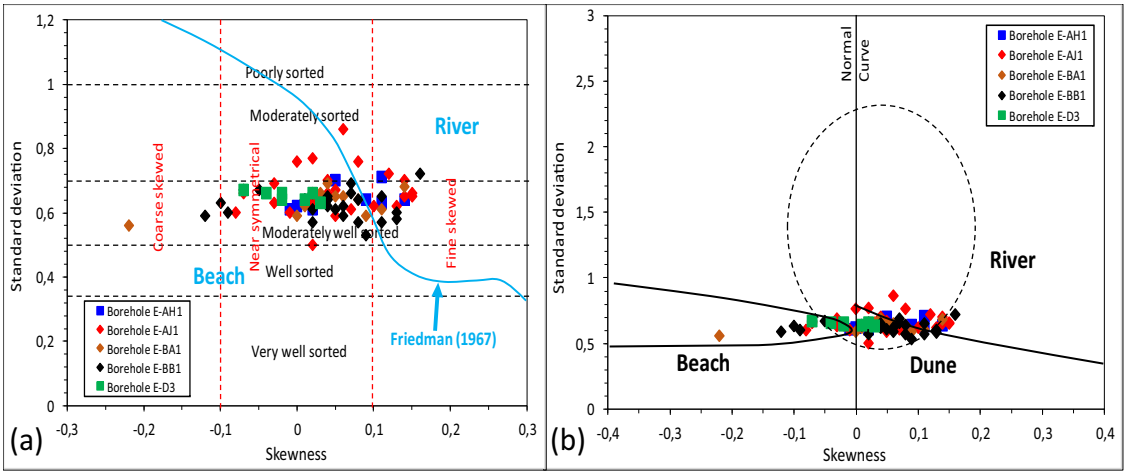

Figure 8: Bivariate plot of skewness vs standard deviation of sandstones from the Bredasdorp Basin showing (a) grain sizes, kurtosis category and depositional environment (background map after ref. [9,30]) and (b) placement of the samples in the fields of beach, dune and river environmentser [9].

demonstrated an excellent correlation with various depositional processes and environments [31]. Sahu [31] used LDFs of Y_1, Y_2, Y_3 and Y_4 to distinguish between shallow agitated water and beach, beach and shallow marine, shallow marine and deltaic or lacustrine and turbidity and deltaic, respectively. The mathematical expression for Y_1, Y_2, Y_3 and Y_4 are presented in equations. In the equations, M, r, SK and KG represent mean grain size, standard deviation, skewness and kurtosis, respectively.

$$Y_1 = -3.5688M + 3.7016r^2 - 2.0766\text{SK} + 3.1135\text{KG} \quad \text{(i)}$$

If Y_1 is greater than – 2.7411, the environment is beach, and if Y_1 is less than – 2.7411, the environment is shallow agitated water.

$$Y_2 = 15.6534M + 65.7091r^2 + 18.1071\text{SK} + 18.5043\text{KG} \quad \text{(ii)}$$

The environment is shallow marine if Y_2 is greater than – 63.3650, and if Y_2 is less than – 63.3650, the environment is beach.

$$Y_3 = 0.2852M - 8.7604r^2 - 4.8932\text{SK} + 0.0482\text{KG} \quad \text{(iii)}$$

If Y_3 is greater than – 7.4190, the environment is shallow marine and if Y_3 is less than – 7.4190, the environment is lacustrine or deltaic.

$$Y_4 = 0.7215M - 0.4030r^2 + 6.7322\text{SK} + 5.2927\text{KG} \quad \text{(iv)}$$

If Y_4 is greater than 9.8433, it suggests deltaic deposition, and if Y_4 is less than 9.8433, it signify turbidity current deposition.

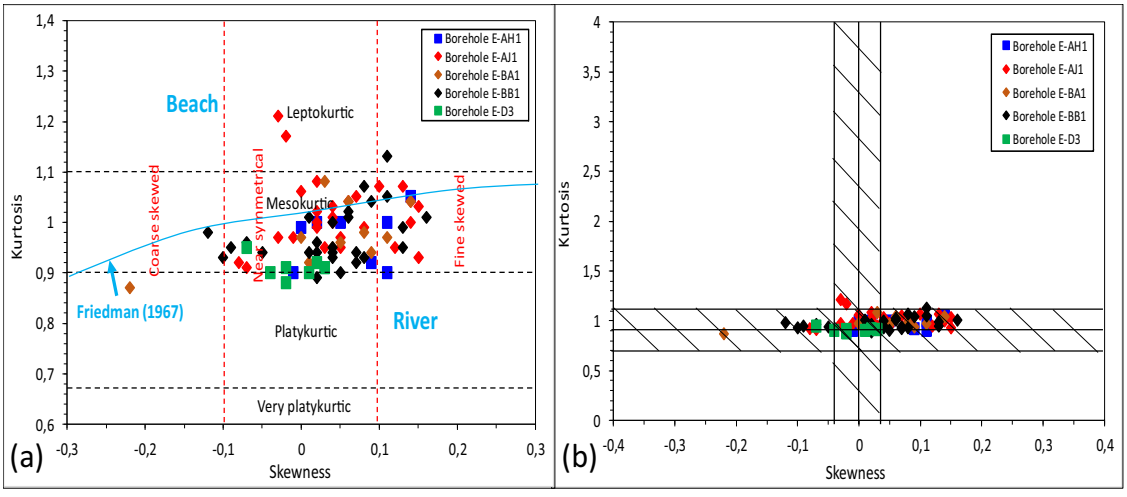

Figure 9: Bivariate plot of skewness vs kurtosis of sandstones from the Bredasdorp Basin showing (a) grain sizes, kurtosis category and depositional environment (background map [9,30]) and (b) placement of the samples in the normal path of sinusoidal trend [29].

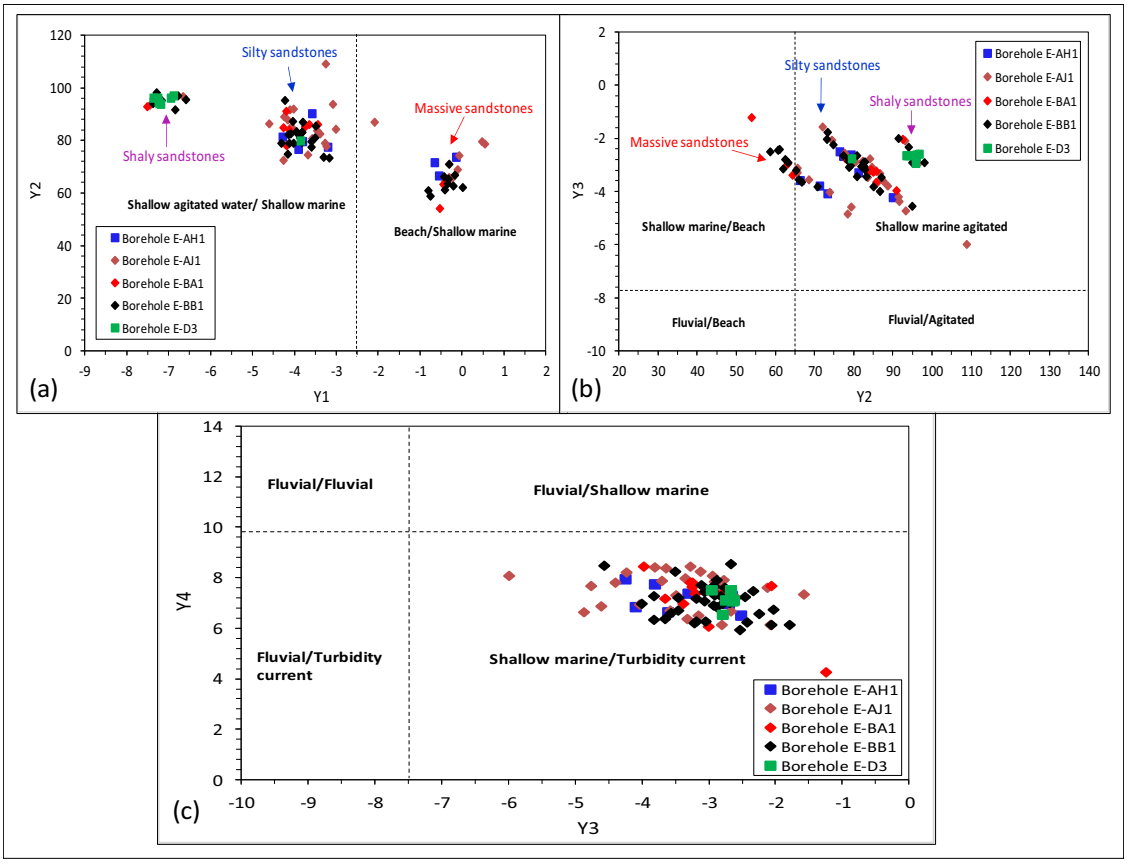

Figure 10: Linear discrimination function (LDF) binary plot of (a) Y_1 against Y_2; (b) Y_2 against Y_3; (c) Y_3 against Y_4, showing depositional environments and processes for the Bredasdorp sandstones (after ref. [31]).

The calculated Y_1, Y_2, Y_3 and Y_4 values for the Bredasdorp sandstones vary from −7.50 to 0.48, 54.01 to 108.85, −6.00 to −1.24 and 5.92 to 8.54, respectively (Table S2 in the supplementary data). The Y_1 values from Boreholes E-AH1, E-AJ1, E-BA1 and E-BB1 show that the massive sandstones are beach process, whereas the shaly and silty sandstones are of agitated water process. With regard to the Y_2 values, all the shaly and silty sandstones fall in the shallow marine environments, while about 65% of the massive sandstones plotted in the shallow marine environment and the remaining 35% plotted in the beach. In terms of Y_3 and Y_4 values, all the analysed samples were plotted in the shallow marine environment and turbidity current deposits, respectively. Also, the bivariate plot of Y_2 against Y_1 (Figure 10a) shows that most of the samples (about 80%) falls in the shallow agitated water area, about 12% plotted in the beach/shallow agitated water area and the remaining samples (about 8%) fall in the beach/beach environment. Figure 10b revealed that approximately 90% of the samples are of shallow agitated marine, whereas about 10% are of shallow marine/beach environment. The binary plot of Y_4 against Y_3 revealed that the Bredasdorp sandstones are shallow water marine/turbidity current deposits (Figure 10c). The linear arrangement of the samples into three groups could be due to marine regression. The deduced depositional environment in this study are comparable or support the depositional interpretation of the Bredasdorp Basin as reported by Brown et al. [18], McMillan et al. [24] and Broad et al. [26] using facies and seismic analyses. According to McMillan et al. [24], during the rifting phase when half-graben basin styles were dominant, sediments accumulated in a wide range of environments (non-marine to slope). In the Bredasdorp Basin, where major bounding faults are less developed, sediments were laid down in non-marine and marginal marine environment, resulting in widespread development of red and green claystones overlain by clean, porous glauconitic littoral sandstones.

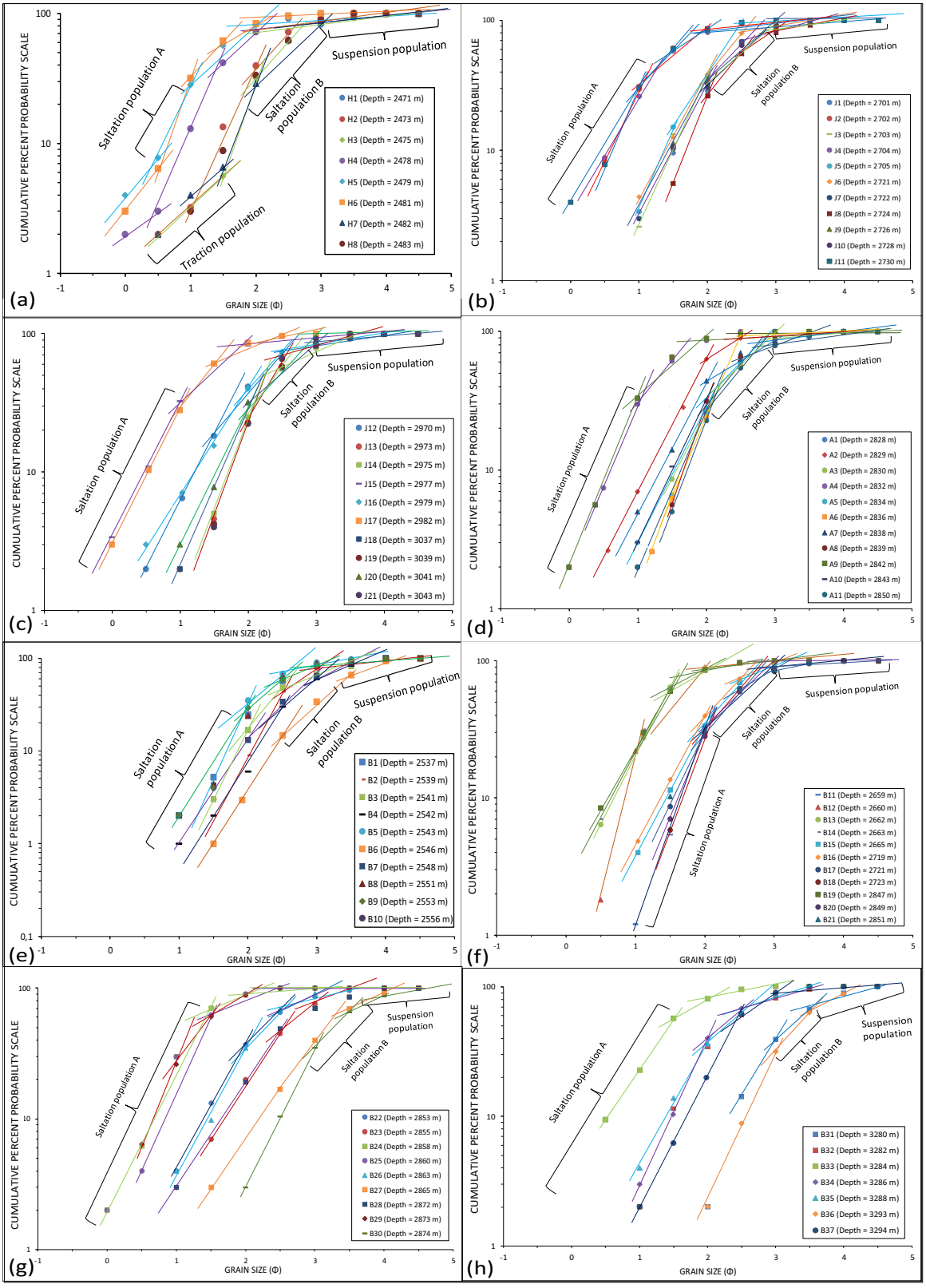

Figure 11: Log–probability weight percentage frequency curves showing the double saltation and single suspension and traction populations for (a) Borehole E-AH1; (b and c) Borehole E-AJ1; (d) Borehole E-BA1; (e–g) Borehole E-BB1; (h) Borehole E-D3.

Table 4: Lithofacies and their associated graphic grain size parameters

Borehole	Core no.	Lithofacies	Depth (m)	Ø1	Ø5	Ø16	Ø25	Ø50	Ø75	Ø84	Ø95	C (μm)	M (μm)
E-AH1	1	Silty sandstone	2,471.00	1.05	1.28	1.65	1.84	2.30	2.81	3.05	3.65	699.88	200.52
		Silty sandstone	2,473.00	0.66	1.10	1.54	1.71	2.15	2.56	2.78	3.15	1,033.70	232.97
		Silty sandstone	2,475.00	1.10	1.46	1.70	1.87	2.30	2.78	2.99	3.46	665.74	200.52
		Massive sandstone	2,478.00	0.20	0.55	0.82	1.03	1.40	1.85	2.09	2.66	1,637.46	493.19
		Massive sandstone	2,479.00	0.05	0.33	0.70	0.92	1.38	1.87	2.08	2.64	1,902.46	503.16
		Massive sandstone	2,481.00	0.08	0.39	0.69	0.88	1.30	1.80	2.00	2.46	1,846.23	545.06
		Silty sandstone	2,482.00	1.09	1.35	1.71	1.91	2.31	2.73	2.92	3.35	672.43	198.52
		Silty sandstone	2,483.00	1.06	1.28	1.65	1.82	2.28	2.73	2.89	3.27	692.91	204.57
E-AJ1	1	Silty sandstone	2,701.30	1.05	1.25	1.66	1.90	2.28	2.70	2.92	3.35	699.88	204.57
		Massive sandstone	2,702.50	0.06	0.29	0.68	0.89	1.32	1.80	1.98	2.50	1,883.53	534.27
		Silty sandstone	2,703.00	0.76	1.11	1.55	1.74	2.19	2.61	2.81	3.17	935.33	223.83
		Massive sandstone	2,704.00	0.07	0.29	0.70	0.97	1.38	1.88	2.11	2.58	1,864.79	503.16
		Silty sandstone	2,705.00	0.69	1.06	1.52	1.72	2.22	2.68	2.85	3.20	1,003.15	217.22
	2	Silty sandstone	2,721.00	0.60	1.13	1.70	2.03	2.50	3.14	3.45	3.95	1,097.62	164.17
		Silty sandstone	2,722.00	0.80	2.10	2.52	2.70	3.14	3.57	3.82	4.24	898.66	86.57
		Silty sandstone	2,724.00	1.09	1.46	1.76	1.98	2.40	2.90	3.20	3.70	672.43	181.44
		Silty sandstone	2,726.00	1.05	1.22	1.59	1.78	2.24	2.71	2.93	3.42	699.88	212.92
		Silty sandstone	2,728.00	1.04	1.23	1.62	1.83	2.28	2.70	2.85	3.18	706.91	204.57
		Massive sandstone	2,730.00	0.06	0.32	0.68	0.87	1.32	1.78	1.96	2.44	1,883.53	534.27
	3	Silty sandstone	2,970.00	0.68	1.20	1.55	1.77	2.29	2.86	3.01	3.83	1,013.23	202.53
		Silty sandstone	2,973.00	1.05	1.51	1.8	2.03	2.39	2.88	3.16	3.64	699.88	183.26
		Silty sandstone	2,975.00	1.55	1.56	1.80	2.00	2.40	2.90	3.16	3.61	424.50	181.44
		Massive sandstone	2,977.00	0.00	0.08	0.55	0.79	1.32	1.85	2.08	2.66	2,000.00	534.27
		Silty sandstone	2,979.00	0.30	0.85	1.52	1.70	2.15	2.53	2.79	3.3	1,481.64	232.97
		Massive sandstone	2,982.00	0.07	0.34	0.70	0.92	1.33	1.78	1.96	2.41	1,864.79	528.95
	4	Silty sandstone	3,037.000	1.10	1.51	1.81	2.03	2.39	2.87	3.10	3.65	665.74	183.26
		Silty sandstone	3,039.00	1.12	1.50	1.82	2.04	2.39	2.84	3.04	3.58	652.56	183.26
		Silty sandstone	3,041.00	1.07	1.32	1.67	1.86	2.24	2.64	2.88	3.32	686.02	212.92
		Silty sandstone	3,043.00	1.14	1.52	1.82	2.02	2.32	2.68	2.84	3.16	639.64	196.55
	5	Silty sandstone	2,692.00	1.12	1.46	1.73	1.92	2.33	2.75	2.92	3.39	652.56	194.59
		Shaly sandstone	2,695.00	2.04	2.32	2.70	2.91	3.31	3.73	3.91	4.27	260.06	73.03
		Silty sandstone	2,698.00	1.08	1.37	1.70	1.89	2.36	2.88	3.19	3.66	679.19	188.84
		Silty sandstone	2,701.00	1.08	1.18	1.68	1.94	2.30	2.70	2.92	3.35	679.19	200.52
		Silty sandstone	2,705.00	1.10	1.52	1.80	2.01	2.37	2.82	3.01	3.63	665.74	186.96
		Massive sandstone	2,708.00	0.07	0.07	0.64	0.92	1.37	1.89	2.16	2.58	1,864.79	508.21
E-BA1	1	Silty sandstone	2,828.00	1.08	1.43	1.76	1.98	2.36	2.84	3.06	3.48	679.19	188.84
		Shaly sandstone	2,829.00	2.06	2.36	2.71	2.92	3.31	3.72	3.90	4.26	254.91	73.03
		Silty sandstone	2,830.00	1.06	1.29	1.70	1.94	2.34	2.79	2.98	3.52	692.91	192.66
		Massive sandstone	2,832.00	0.07	0.34	0.69	0.90	1.32	1.78	1.96	2.32	1,864.79	534.27
		Silty sandstone	2,834.00	1.09	1.36	1.72	1.94	2.35	2.81	3.00	3.57	672.43	190.74
	2	Silty sandstone	2,836.00	1.1	1.4	1.78	2.01	2.41	2.9	3.12	3.49	665.74	179.63
		Massive sandstone	2,838.00	0.12	0.52	0.71	0.86	1.49	1.68	1.88	2.26	1,773.84	450.75
		Silty sandstone	2,839.00	1.08	1.45	1.70	1.88	2.28	2.71	2.92	3.36	679.19	204.57
		Massive sandstone	2,842.00	0.09	0.42	0.68	0.85	1.26	1.71	1.90	2.46	1,827.86	567.31
		Silty sandstone	2,843.00	1.05	1.24	1.62	1.85	2.31	2.82	3.04	3.48	699.88	198.52
		Silty sandstone	2,850.00	1.09	1.50	1.82	2.04	2.43	2.91	3.20	3.70	672.43	176.07
E-BB1	1	Silty sandstone	2,537.20	1.09	1.48	1.78	2.00	2.39	2.85	3.08	3.65	672.43	183.26
		Silty sandstone	2,537.70	1.09	1.50	1.78	2.00	2.40	2.84	3.00	3.58	672.43	181.44
	2	Silty sandstone	2,539.00	1.10	1.51	1.80	2.02	2.44	2.96	3.28	3.82	665.74	174.32
		Silty sandstone	2,541.00	1.09	1.37	1.73	1.97	2.38	2.83	3.00.	3.49	672.43	185.10
		Silty sandstone	2,543.00	1.08	1.38	1.72	1.92	2.36	2.84	3.03	3.47	679.19	188.84
		Silty sandstone	2,546.00	1.08	1.43	1.66	1.83	2.22	2.66	2.88	3.35	679.19	217.22
		Shaly sandstone	2,548.00	1.71	2.10	2.54	2.77	3.24	3.67	3.83	4.14	361.73	78.33
		Shaly sandstone	2,551.00	1.61	2.05	2.56	2.78	3.26	3.72	3.89	4.26	399.78	76.78
		Silty sandstone	2,553.00	1.12	1.51	1.79	2.02	2.32	2.73	2.90	3.46	652.56	196.55
		Silty sandstone	2,556.00	1.09	1.34	1.70	1.90	2.34	2.82	3.01	3.48	672.43	192.66

Table 4: Continued

Borehole	Core no.	Lithofacies	Depth (m)	Ø1	Ø5	Ø16	Ø25	Ø50	Ø75	Ø84	Ø95	C (μm)	M (μm)
	3	Silty sandstone	2,659.00	0.90	1.45	1.72	1.89	2.25	2.67	2.90	3.34	813.14	210.80
		Massive sandstone	2,660.00	0.23	0.58	0.86	1.04	1.36	1.75	1.90	2.38	1,589.07	513.32
		Massive sandstone	2,662.00	0.09	0.40	0.73	0.94	1.30	1.74	1.90	2.39	1,827.86	545.06
		Massive sandstone	2,663.00	0.08	0.34	0.68	0.86	1.28	1.76	1.98	2.39	1,846.23	556.07
		Silty sandstone	2,665.00	0.64	1.13	1.60	1.82	2.24	2.62	2.79	3.04	1,054.58	212.92
	4	Silty sandstone	2,719.00	0.62	1.08	1.51	1.72	2.16	2.54	2.74	2.99	1,075.89	230.65
		Silty sandstone	2,721.00	1.03	1.29	1.66	1.85	2.29	2.80	3.01	3.43	714.01	202.53
		Silty sandstone	2,723.00	1.09	1.44	1.72	1.90	2.34	2.79	2.98	3.40	672.43	192.66
	5	Massive sandstone	2,847.00	0.06	0.30	0.68	0.88	1.33	1.80	1.97	2.42	1,883.53	528.95
		Silty sandstone	2,849.00	1.06	1.37	1.70	1.92	2.34	2.79	2.97	3.50	692.91	192.66
		Silty sandstone	2,851.00	2.05	2.26	2.64	2.85	3.3	3.78	3.97	4.40	257.47	73.77
		Silty sandstone	2,853.00	1.03	1.19	1.58	1.75	2.23	2.74	2.95	3.46	714.01	215.06
		Massive sandstone	2,855.00	0.03	0.20	0.56	0.73	1.17	1.61	1.83	2.22	1,940.89	620.73
		Massive sandstone	2,858.00	0.08	0.40	0.71	0.90	1.25	1.62	1.87	2.28	1,846.23	573.01
		Massive sandstone	2,860.00	0.10	0.44	0.72	0.90	1.31	1.73	1.90	2.25	1,809.67	539.64
		Silty sandstone	2,863.00	1.05	1.26	1.60	1.80	2.22	2.64	2.85	3.23	699.88	217.22
		Shaly sandstone	2,865.00	1.61	2.03	2.46	2.68	3.18	3.63	3.84	4.20	399.78	83.17
	6	Massive sandstone	2,872.00	0.04	0.24	0.62	0.80	1.26	1.75	1.97	2.40	1,921.58	567.31
		Silty sandstone	2,872.80	1.05	1.26	1.63	1.81	2.26	2.72	2.92	3.30	699.88	208.70
		Massive sandstone	2,873.00	0.08	0.39	0.74	0.97	1.35	1.76	1.92	2.30	1,846.23	518.48
		Shaly sandstone	2,873.80	2.04	2.25	2.62	2.80	3.25	3.72	3.93	4.31	260.06	77.55
	8	Shaly sandstone	3,280.40	2.03	2.18	2.54	2.71	3.18	3.67	3.88	4.26	262.67	83.17
		Silty sandstone	3,282.00	1.04	1.22	1.60	1.79	2.29	2.84	3.08	3.48	706.91	202.53
		Massive sandstone	3,284.00	0.06	0.28	0.68	0.92	1.38	1.88	2.12	2.49	1,883.53	503.16
		Silty sandstone	3,286.00	1.03	1.16	1.50	1.69	2.18	2.68	2.90	3.29	714.01	226.08
		Silty sandstone	3,288.00	1.03	1.18	1.55	1.74	2.24	2.73	2.90	3.28	714.01	212.92
		Shaly sandstone	3,292.70	2.05	2.28	2.66	2.86	3.30	3.74	3.92	4.30	257.47	73.77
		Silty sandstone	3,294.00	1.08	1.40	1.70	1.89	2.31	2.73	2.89	3.25	679.19	198.52
E-D3	1	Shaly sandstone	3,261.20	2.05	2.22	2.60	2.82	3.31	3.78	3.96	4.32	257.47	73.03
		Shaly sandstone	3,262.90	2.04	2.22	2.60	2.80	3.30	3.78	3.97	4.33	260.06	73.77
		Shaly sandstone	3,266.50	2.03	2.17	2.52	2.71	3.19	3.66	3.87	4.30	262.67	82.34
		Shaly sandstone	3,268.00	2.04	2.20	2.58	2.75	3.22	3.69	3.88	4.26	260.06	79.91
		Shaly sandstone	3,269.00	2.04	2.20	2.58	2.74	3.20	3.66	3.86	4.24	260.06	81.52
	2	Shaly sandstone	3,526.00	2.04	2.20	2.56	2.74	3.18	3.64	3.86	4.20	260.06	83.17
		Silty sandstone	3,528.50	1.06	1.28	1.66	1.86	2.32	2.78	2.96	3.33	692.91	196.55
		Shaly sandstone	3,529.50	1.63	2.07	2.58	2.78	3.28	3.74	3.92	4.29	391.86	75.26

Where C and M represent the coarser one-percentile value (in micron) and median (in micron), respectively.

4.6 Log–probability curves and depositional processes

The log–probability curves [12] were used to distinguish between traction, saltation and suspension load in the Bredasdorp sediments. The Visher plot for the Borehole sandstones in Boreholes E-AH1, E-AJ1, E-BA1, E-BB1 and E-D3 (Figure 11) revealed the predominance of double saltation (saltations I and II) populations with only one suspension population. The saltation and suspension populations may range up to 80 and 20%, respectively. The saltation I and II populations often truncated between 1.5∅ and 2.5∅, which could be ascribed to internal forces that are initiating rolling or sliding along sea floor [12]. The saltation I and II populations are moderately well-sorted when compared to the suspension population. In fact, the suspension load was not sorted during deposition, and it was deposited by gravity sinking from suspension mud. The log probability curves (Figure 11) are similar to ancient and modern marine sediments as envisaged by Visher [12], wherein both saltation (saltations I and II) and suspension populations prevailed. Two saltation populations are usually related to tidal environment of active flow and ebb currents at the same time.

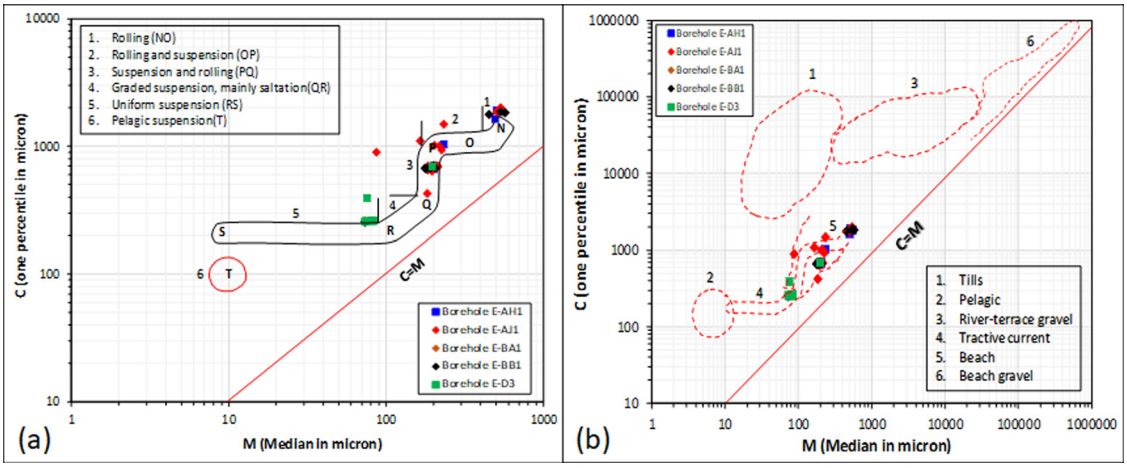

Figure 12: Binary plot of C–M values in Table 4 on the Passega diagram, showing (a) the mode of transportation and (b) depositional process for the Bredasdorp sandstones (after ref. [40]).

4.7 The C–M pattern (Passega diagram)

The C–M plot was initiated by Passega [40] to interpret the hydrodynamic conditions that prevail during the deposition of sediments. The C–M is a bivariate plot of the median value (M) in micron vs coarser one-percentile value (C) in micron on a log–probability scale (Table 4). The connection between C and M is related to the energy of the transportation medium as well as the nature and type of the sediment [12]. The Passega diagram illustrated in Figure 12a revealed quite a few fields of rolling and suspension, corresponding to the different transportation and sedimentation conditions in the shallow marine envi ronments. The binary plot of C against M values (Table 4) on the Passega diagram suggests that samples from Borehole E-AH1 plotted in both rolling (NO) and rolling and suspension (OP), Borehole E-AJ1 are scattered in the rolling (NO), rolling and suspension (OP) as well as in the suspension and rolling (PQ) sections, while samples from Borehole E-BA1 fall within the suspension and rolling (PQ) category (Figure 12a). Samples from Borehole E-BB1 are plotted in both rolling (NO) and suspension and rolling (PQ), whereas most of the samples from Borehole E-D3 fall in the uniform suspension category (RS). The background C–M plot (Figure 12b) by Passega [40] shows that the studied samples are tractive current and beach deposits.

5 Conclusions

The present study reveals that different textural characteristics of sediments can give vital clues to understanding their depositional environments as well as the mechanisms of transportation. The present Bredasdorp samples have been interpreted based on the evidences provided mostly by the grain size distribution curves, bivariate plots, LDF, log–probability curves and Passega diagram (C–M pattern). The grain size distribution shows that the Bredasdorp sandstones are mostly fine-grained, moderately well-sorted, mesokurtic and near symmetrical. The fine sand nature of sediments points to the fact that moderately low-energy condition dominates in the study area. The well-sorted to moderately well-sorted nature of the sediments suggests an abrupt winnowing and back and forth movement by the depositing agents. The dominance of near symmetrical category perhaps indicates riverine input and mixing of similar modal fractions. The unimodal distribution of the sediments shows the stable depositional process during which the Bredasdorp sediments were laid down. The LDF analysis reveals that the sediments are turbidity current deposits under coastal dune and beach process in a shallow marine environment. The C–M pattern (Passega diagram) signifies that the Bredasdorp sediments were mostly deposited by rolling, rolling and suspension, suspension and rolling and uniform suspension. Furthermore, the Passega diagram shows that the studied sandstones are chiefly deposited by beach process. The log–probability weight percentage frequency curves revealed that the sediments were primarily affected by tidal flow and ebb currents during their deposition.

Acknowledgements: The authors are grateful to the National Research Foundation-Southern African Systems Analysis Centre (NRF-SASAC; UID: 118768) and the DSI-NRF Centre of Excellence (CoE) for Integrated Mineral and Energy Resource Analysis (CIMERA) for financial support. The

Petroleum Agency of South Africa (PetroSA) and the Govan Mbeki Research and Development Centre (GMRDC) of the University of Fort Hare are appreciated for granting access to the cores and logistic supports, respectively.

References

[1] Srivastava AK, Ingle PS, Lunge HS, Khare N. Grain-size characteristics of deposits derived from different glaciogenic environments of the Schirmacher Oasis, East Antarctica. Geologos. 2012;18(4):251–66.
[2] Baiyegunhi C, Liu K, Gwavava O. Grain size statistics and depositional pattern of the Ecca Group sandstones, Karoo Supergroup in the Eastern Cape Province, South Africa. Open Geosci. 2017;9:554–76.
[3] Blott SJ, Pye K. Radistat: A grain size distribution and statistics package for the analysis of unconsolidated sediments. Earth Surf Process Landf. 2001;26:1237–48.
[4] Bui EN, Mazullo J, Wilding LP. Using quartz size and shape analysis to distinguish between aeolian and fluvial deposits in the Dllot Bosso of Niger (West Africa). Earth Surf Process Landf. 1990;14:157–66.
[5] Edwards AC. Grain size and sorting in modern beach sands. J Coast Res. 2001;17:38–52.
[6] Goswami B, Ghosh D. Understanding the transportational and depositional setting of Panchet Formation, Purulia and Bankura districts of West Bengal, India - Evidence from grain size analysis. Front Earth Sci. 2011;5(2):138–49.
[7] Srivastava AK, Ingle PS, Lunge HS, Khare N. Grain-size characteristics of deposits derived from different glacigenic environments of the Schirmacher Oasis, East Antarctica. Geologos. 2012;18(4):251–66.
[8] Stanley-Wood N, Lines RW. Particle size analysis. Cambridge: Royal Society of Chemistry, Special Publication; 1992. p. 101–3.
[9] Friedman GM. Dynamic processes and statistical parameters compared for size frequency distribution of beach and river sands. J Sediment Petrology. 1967;37:327–54.
[10] Friedman GM. Differences in size distribution of populations of particles among sands of various origin. Sedimentology. 1979;26:859–62.
[11] Moiola RJ, Weiser D. Textural parameters: An evaluation. J Sediment Petrol. 1968;38:45–53.
[12] Visher GS. Grain size distributions and depositional processes. J Sediment Petrol. 1969;39:1074–106.
[13] Sagoe KMO, Visher GS. Population breaks in grain-size distributions of sand – a theoretical model. J Sediment Pet. 1977;47(1):285–310.
[14] Sonibare WA. Structure and evolution of basin and petroleum systems within a transform- related passive margin setting: Data-based insights from crust-scale 3D modelling of the Western Bredasdorp Basin, offshore South Africa. PhD thesis. University of Stellenbosch; 2015. p. 16–44.
[15] Liro LM, Dawson WC. Reservoir systems of selected basins of the South Atlantic. In: Mello MR and Katz BJ, editors, Petroleum system of South Atlantic margins. vol. 73. United States: American Association of Petroleum Geologists Memoir; 2000. p. 77–92.
[16] Burden PLA, Davies CPN. Exploration to first production on block 9 off South Africa. Oil Gas J. 1997;1:92–98.
[17] Tinker J, de Wit M, Brown R. Linking source and sink: Evaluating the balance between onshore erosion and offshore sediment accumulation since Gondwana break-up, South Africa. Tectonophysics. 2008;455(1):94–103.
[18] Brown LF, Brink JM, Doherty GJ, Jollands S, Jungslager A, Keenan EHA, et al. Sequence stratigraphy in offshore South African divergent basins. Am. Ass. Petrol. Geol., Studies in Geology. vol. 41. United States: An Atlas on Exploration for Cretaceous Lowstand traps, by Soeker (Pty) Ltd; 1995. p. 83–131.
[19] Burden PLA. Soekor partners explore possibilities in Bredasdorp Basin off South Africa. Oil Gas J. 1992;90(51):109–12.
[20] Davies CPN. Hydrocarbon evolution of the Bredasdorp Basin, offshore South Africa—From source to reservoir. University of Stellenbosch. PhD dissertation; 1997. p. 1123.
[21] Petroleum Agency of South Africa, PASA. Petroleum Exploration Information and Opportunities: Petroleum Agency South Africa Brochure, 2005, (www.petroleumagencysa.com/files/information).
[22] Schalkwyk HJM, Assessment controls on reservoir performance and the effects of granulation seam mechanics in the Bredasdorp Basin, South Africa. MSc thesis. South Africa: University of the Western Cape; 2005. p. 128
[23] Turner JR, Grobber N, Sontundu S. Geological modelling of the Aptian and Albian sequences within Block 9, Bredasdorp Basin, Offshore South Africa. In: Kisters AFM, Thomas RJ, editors. Journal of African Earth Sciences, Geocongress 2000: A new millennium on ancient crust, 27th Earth Science Congress of the Geological Society of South Africa; 2000. p. 80.
[24] McMillan IK, Brink GJ, Broad DS, Maier JJ. Late Mesozoic sedimentary basins off the south coast of South Africa. In: Selley RC, editors. Sedimentary basins of the world—African basins. Amsterdam: Elsevier Science B.V.; 1997. p. 319–376.
[25] De Wit MJ, Ransome IG. Regional inversion tectonics along the southern margin of Gondwana. In: De Wit MJ, Ransome IG, editors. Inversion tectonics of the Cape Fold Belt, Karoo and Cretaceous Basins of Southern Africa. Rotterdam; 1992. p. 15–22.
[26] Broad DS, Jungslager EHA, McLachlan IR, Roux J. Offshore Mesozoic basins. In: Johnson MR, Anhaeusser CR, Thomas RJ, editors. The geology of South Africa. Geological Society of South Africa. Pretoria: Johannesburg/Council for Geoscience; 2006. p. 553–71.
[27] Johnson MR. Thin section grain size analysis revisited. Sedimentology. 1994;41:985–99.
[28] Kendall M, Stuart A. The advanced theory of statistics. Distribution theory *Griffin London*. vol. 1; 1958. p. 325.
[29] Folk RL, Ward W. Brazos river bar: A study in the significance of grain size parameters. J Sediment Petrology. 1957;27: 3–26.
[30] Folk RL. Petrology of sedimentary rocks. Austin TX: Hemphill Publishing Co.; 1974. p. 182.

[31] Sahu BK. Depositional mechanism from the size analysis of elastic sediments. J Sediment petrology. 1964;34(1):73–83.
[32] Ramanathan AL, Rajkumar K, Majumdar J, Singh G, Behera PN, Santra SC, et al. Textural characteristics of the surface sediments of a tropical mangrove Sundarban ecosystem. India Indian Journ Mar Sci. 2009;38(4):397–403.
[33] Duane DB. Significance of skewness in recent sediments, western Pamlico Sound, North Carolina. J Sediment Petrol. 1964;34(4):864–74.
[34] Stewart HB. Sedimentary reflection on depositional environment, in San Mignellagoon, Baju California, Mexico. AAPG Bull. 1958;42:2567–618.
[35] Al-Ghadban AN. Holocene sediments in a shallow bay, southern coast of Kuwait. Arab Gulf Mar Geol. 1990;92:237–54.
[36] Sutherland RA, Lee C. Discrimination between coastal subenvironments using textural characteristics. Sedimentology. 1994;41:1133–45.
[37] Srivastava AK, Khare N, Ingle PS. Textural characteristics, distribution pattern and provenance of heavy minerals in glacial sediments of Schirmacher Oasis, East Antarctica. J Geol Soc India. 2010;75:393–402.
[38] Griffiths JC. Size-frequency distribution of detrital sediments based on sieving and pipette sedimentation. (Abstract). Bull Geol Soc Am. 1967;68:17–39.
[39] Friedman GM. Distinction between dune, beach and river sands from their textural characteristics. J Sediment Petrol. 1961;31:514–29.
[40] Passega R. Texture as characteristics of clastic deposition. Am Assoc Pet Geologists Bull. 1957;41:1952–84.